Volume 1 | Number 1 | Jan 2013 | Pages 1–100

PCCP

Physical Chemistry Chemical Physics
www.rsc.org/pccp

ROYAL SOCIETY OF CHEMISTRY

ROYAL SOCIETY OF CHEMISTRY

www.rsc.org/pccp

Ionogel approach harnesses ionic liquid's properties and strikingly enhances them. Confined ionic liquid shows high fragility and good lithium transport, in relation to silica interface.
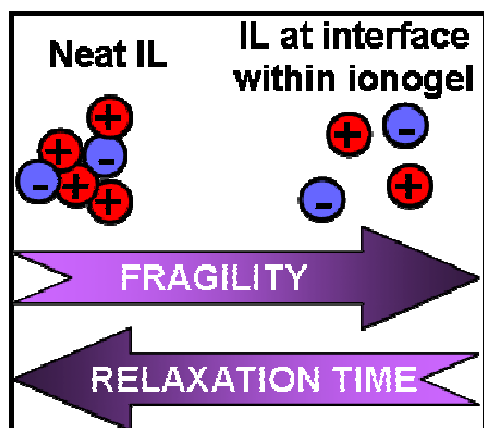
ARTICLE TYPE

Destructuring ionic liquids in ionogels: enhanced fragility for solid devices

A. Guyomard-Lack,[a] P-E. Delannoy,[a] N. Dupré,[a] C. V. Cerclier,[a] B. Humbert [a] and J. Le Bideau[a]*

Confining ionic liquids (ILs) with added lithium salt within silica host networks enhances their fragility and improves their conductivity. Overall conductivity measurements, Raman spectroscopy on TFSI anion and NMR spectroscopy on lithium cation, show segregative interaction of lithium ions with the SiO_2 host matrix. This implies at IL / SiO_2 interfaces a breakdown of aggregated regions that are found
10 systematically in bulk ILs. Such a destructuration due to interface effect determines the fragility and thus results locally at the interface in short relaxation times, low viscosity, and good ionic conductivity. The "destructuration" of ions pairs or domains in the ILs makes ILs within ionogels a competitive alternative to existing solid ionic conductors in all-solid devices, such as lithium batteries and supercapacitors.

Introduction

15 Ionic liquids (ILs) are commonly used room-temperature (RT) molten salts with a unique combination of properties including a wide electrochemical window, good ionic conductivity, good chemical and thermal stability, and very low volatility. These properties make them attractive for many industrial processes and
20 domestic applications such as liquid-liquid extraction, catalysis, energy storage and electro- and photo-chromism.[1-3] More specifically, they are seen as a potential replacement for traditional volatile organic compounds (VOC) used in solar cells, double layer capacitors and lithium batteries[4]: however, since ILs
25 are liquids at room temperature they fail to compete effectively with VOC-based devices.

   Several strategies exist to immobilize ILs for use in all-solid devices. We have focused our attention on the confinement of ILs within host networks with a continuous silica interface, resulting
30 in chemical gels, namely ionogels; specifically in the present paper, the host network is made only of mesoporous silica. This method of ionogels synthesis, via the sol-gel routes, is well-established, including different procedures to obtain different pore sizes and shapes.[5] It has been shown that in these materials
35 exhibiting 60 to 95 *vol*% of IL ("polymer-in-salt"), the confinement preserved the liquid dynamics and allowed liquid-like behaviour for real all-solid devices, at RT as well as below the solidification temperature of the neat IL.[6-8] Ionogels allow to be shaped as solids, preserving simultaneously the liquid
40 properties.

   Ionogels were shown to work effectively as solid electrolytes in lithium batteries.[9] Nevertheless, addition of lithium to the IL is known to increase its viscosity and decrease its conductivity.[9] Studies on viscosity of confined ILs by means of physical
45 apparatus external to the material have been reported.[11] The Walden product has been used for years to illustrate this conductivity-viscosity relationship.[12-16] However, the Walden product represents a macroscopic approach: a more microscopic approach based on the possible cation-anion association, from
50 simple pairs up to nano-aggregated strongly interacting domains,

has been proposed. This could be quantified through the ionicity of ILs, which is measured by the ratio between the molar conductivity measured by complex impedance spectroscopy (CIS) (macroscopic level) and by NMR (molecular level)
55 ($\Lambda_{imp}/\Lambda_{NMR}$).[17] NMR measurement probes the diffusion of each ion, associated or not with another, whereas CIS, which implies an electric field, probes the diffusion of each charged species, mostly single ions, and insignificantly associated ions. Thus the $\Lambda_{imp}/\Lambda_{NMR}$ ratio may give information on the fraction of non-
60 associated cations and anions.[18,19]

   It remains a challenge to reduce ILs' viscosities and increase their conductivities. We show herein that confining ILs in silica based ionogels allows furthering this goal as well as offering a route to all-solid devices. We show the effect of the silica
65 interface on Li^+ coordination and dynamics, on lithium cation transference number (t_{Li+}) and on conductivity. Vogel-Tamman-Fulcher (VTF) fitting of the thermal dependence of the conductivity allows reaching fragility index. By increasing the fragility of the confined ILs, we also gain information on the
70 ionicity of ILs confined within silica based ionogels.

Experimental

Electrolytic solution (ES) was obtained by dissolving bis(trifluorosulfonyl)imide lithium salt (LiTFSI, 0.1 g, 3M, 99%) in N-methyl-N-propylpyrrolidinium bis(trifluorosulfonyl)imide
75 (Pyr13TFSI, 1 g, Solvionic, 99.5%). Ionogel were prepared using a non aqueous sol-gel route as previously published:[6] tetramethoxysilane (TMOS, Fluka) and ES were stirred for 10 min and formic acid (F.A., Aldrich, 98 %) (molar ratio F.A. : SiO_2 = 7.8 : 1) was added drop wise under stirring for 2 min. The
80 mixture was then poured into a teflon mould. Gelation was completed at room temperature for 8 days, and all volatile compounds (formic acid, methanol, formate) removed. Transparent monolith was obtained. The porosity of ionogel was analyzed using nitrogen sorption isotherms measured at 77 K
85 (Micromeritics ASAP 2010 sorption instrument). Prior to this
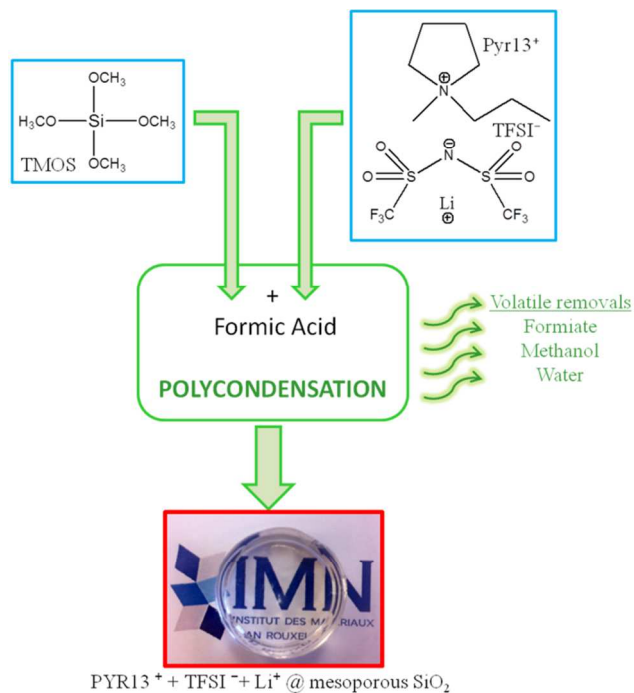
Scheme 1 Synthetic scheme for in-situ sol-gel condensation of alkoxysilane in the presence of Pyr13TFSI and LiTFSI.

analysis, the ionogel samples were outgassed in vacuum at 250°C
5 for at least 48 h. The specific surface area was measured using the BET model and the mesopore size distribution was evaluated BJH method. Transmission electron microscopy was performed on a Hitachi H9000NAR instrument operating at 300 kV. The samples were sliced 100 μm thick with an ultramicrotome. Before
10 DSC measurements (Q20 calorimeter, TA Instrument), samples were dried at 50°C under vacuum for 24h and sealed in hermetic aluminium pans. Samples were then quenched to -150°C at 20 °C.min^{-1} and heated from -150 to 200°C at 10 °C.min^{-1} after having reached thermal equilibrium. Data were analysed with TA
15 Universal Analysis software. The ionic conductivities were determined by complex impedance spectroscopy (CIS) using a BioLogic VMP2-Multichanel Potentiostat by varying the temperature from -20 °C to 90 °C. The frequency range used for impedance measurements was 184 kHz - 20 mHz and the
20 amplitude used was 7 mV. All the samples were vacuum dried at 50 °C during 24 h prior to measurement. Lithium cation transference numbers (t_{Li+}) were determined with symmetric cell (metal Li/ionogel or ES/Li metal) and were measured using the D.C. polarization method. The frequency range for the CIS
25 measurements was 184 kHz-100 mHz, with a 10 mV dc signal. Polarization was performed with a 20 mV dc signal. The lithium cation transference numbers were calculated as:

$$t_{Li^+} = \frac{I_s(\Delta V - R_0 I_0)}{I_0(\Delta V - R_s I_s)} \quad (1)$$

Where ΔV is the polarization potential (20 mV); R_0 is the
30 interfacial resistance of the lithium electrode before polarization; R_s is the interfacial resistance of the lithium electrode after polarization; I_0 is current at the start of polarization, and I_s is the steady-state current at polarization. ^{7}Li solid state static NMR
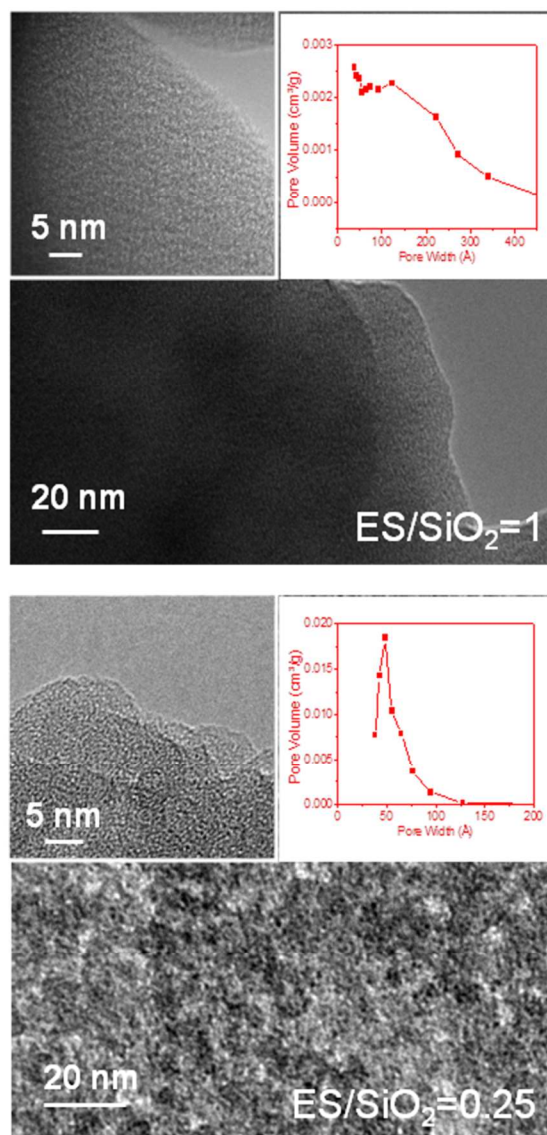

35 **Fig. 1** TEM images of a cross-section of 100 μm of ionogels ES/SiO$_2$=1 and ES/SiO$_2$=0.25, and pore diameter distributions (calculated from the desorption branch of the isotherm using BJH method).

experiments were carried out at room temperature on a Bruker Avance-200 spectrometer (B$_0$ = 4.7T, Larmor frequencies ν_0(^{7}Li)
40 = 77.78 MHz). Pieces of ionic liquid confined in silica matrix were cut and placed into a cylindrical 2.5 mm o.d. zirconia rotor. ^{7}Li static NMR spectra were acquired by making use of a non selective single pulse sequence with π/2=2.3 μs coupled with a pre-acquisition time of 5 μs and a recycle time of 1 s. All spectra
45 displayed in this work were normalized taking into account the number of scans, the received gain, and the mass of sample. ^{7}Li integrated intensities were determined by using spectral simulation (Dmfit software, D. Massiot, http://nmr.cemhti.cnrs-orleans.fr/dmfit/). Raman spectra were recorded on a Bruker
50 Fourier Transform spectrometer, MultiRam device. The 1064 nm line of a Nd : YAG laser was used as excitation source. The laser power was set to 300 mW, the spectral resolution was 2 cm^{-1}, and the inelastic Raman backscattered spectra were obtained as the average of over 200 scans. All the Raman spectra were recorded
55 at room temperature.

Table 1 Surface areas and median pore diameters for different ionogels.

| Sample	Surface area [m².g⁻¹]	Median pore diameter [nm]
ES/SiO₂ = 1	521	17
ES/SiO₂ = 0.5	615	13
ES/SiO₂ = 0.25	582	8
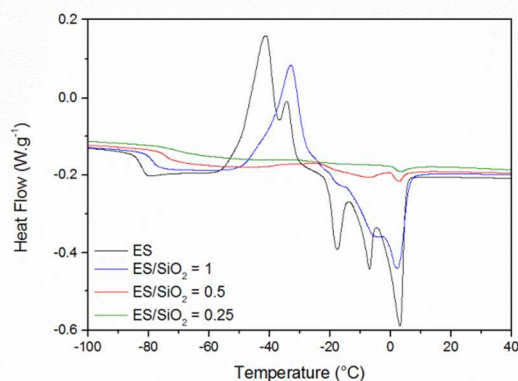
Fig. 2 DSC of (black) neat ES, (blue) ionogel ES/SiO₂ = 1, (red) ionogel ES/SiO₂ = 0.5 and (green) ionogel ES/SiO₂ = 0.25.

Results

The ionogels presented in this study are made of a silica network confining PYR13 TFSI with 0.5M of LiTFSI (Scheme 1). Here, formic acid was used with a constant molar ratio *vs.* TMOS, and the ES:SiO₂:FA molar ratios were 0.25:1:7.8, 0.5:1:7.8 and 1:1:7.8. Depending on the ES:SiO₂:FA molar ratios, gelification is reached within 20 to 60 min. An 8 day aging in an open vial at room temperature allowed completeness of the reaction and removal (evaporation) of formic acid and other side products.[6] Thus in the resulting ionogel, the IL is confined in the porosity. For the sake of characterization of the silica host network, the IL was removed and the porosity was studied by TEM and N₂ sorption isotherms (Fig. 1). This showed an ES/silica bicontinuous interface, *i.e.* a thin silica wall with both interfaces in contact with ES, continuously throughout the ionogels. Table 1 shows that the pore size decreases when ES/SiO₂ decreases and that the surface of the interface is quite stable: this corresponds to an increase of the specific surface per mol of confined ES. Similar values are reported in the literature, and are related to a rough topography of the silica with a fractal character,[20] although it has to be pointed out that the presence of lithium salt may also lead in specific cases to intricate interfaces.[21]

It is important to have clean confined IL for each experiment; to achieve this, each ionogel is vacuum dried at 50°C during 24h.

DSC diagrams are presented Fig. 2. The melting of cold-crystallized ES occurs around 281 K. The two endothermic peaks appearing at lower temperatures could correspond to solid-solid phase transition due to *cisoid* and *transoid* forms or rotation of alkyl chains.[22] As shown by the melting enthalpy $\Delta_m H$ of the confined ES, the part of the confined ES which undergoes crystalline/liquid transition diminishes when ES/SiO₂ decreases (Table 5). This evidences that the quenching of the crystallization by the confinement is more important when the pore size
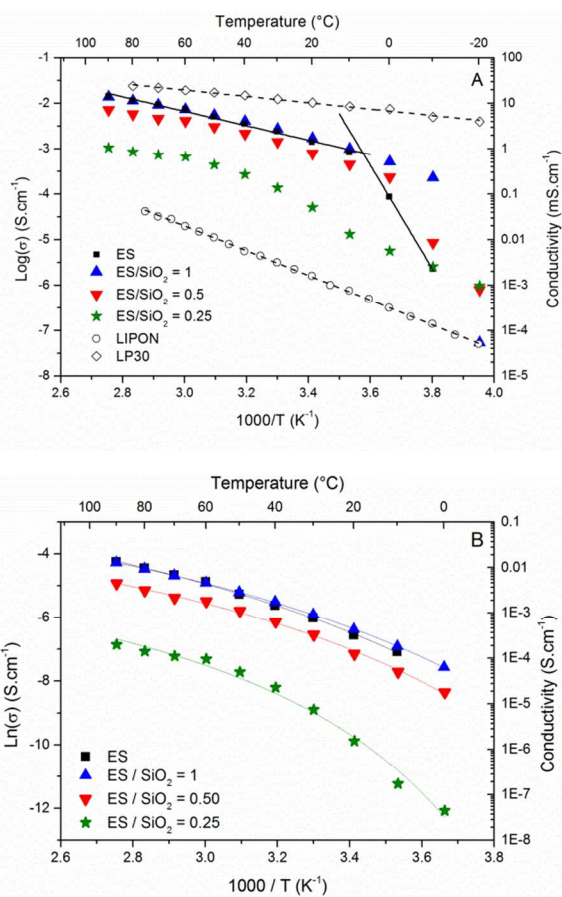
Fig. 3 Conductivity plots, Arrhenius (A) and VTF (B), for neat ES and different ionogels.

diminishes. Moreover, a smaller pore size induces an increase of the glass transition temperature T_g (Table 5).

CIS measurements gives overall ionic transport, *i.e.* a mean value of "bulk" and interface phenomena. Fig. 3A shows the ionic conductivity plots for the different ionogels and for neat ES. For the sake of comparison, the ionic conductivity plots for common electrolytes, *i.e.* liquid LP30 (LiPF₆ in a mixture of ethylene carbonate and dimethyl carbonate, BASF), and solid LiPON (lithium phosphorous oxynitride (Li$_x$PO$_y$N$_z$), are shown. The ionic conductivity of ionogels is considerably higher than that of LIPON and is only slightly lower than that of LP30. The ionogels' conductivity calculations are made on the basis of the same form factor for each sample, *i.e.* they correspond to lower amounts of ES in ionogels than in neat ES: consequently for ionogels, they do not correspond to the intrinsic conductivity of the confined ES but rather to the conductivity of the whole ionogel. Between 10 and 90°C, ionic conductivities of ionogels were only slightly lower than that of neat ES, except in the case of ES/SiO₂ = 0.25 where the low amount of ES has a clear impact on conductivity. When the temperature decreases, conductivity of neat ES decreases suddenly at around 8°C, which is the liquid-solid phase change. The break slope shifted toward lower temperature for ionogels. This break slope appeared less steep when the ES/SiO₂ ratio was lower. The smaller average pore size and the confinement of IL explain both the smaller break slope

Table 2 σ_0, B, T_0 and E_a VTF parameters for different ionogels and ES.

Sample	σ_o [S.cm^{-1}]	B [K]	T_0 [K]	E_a^a [eV]
ES	$4.96 \cdot 10^{-1}$	629	185	0.34
ES/SiO$_2$ = 1	$3.38 \cdot 10^{-1}$	563	186	0.34
ES/SiO$_2$ = 0.5	$1.30 \cdot 10^{-1}$	478	199	0.34
ES/SiO$_2$= 0.25	$0.25 \cdot 10^{-1}$	405	*225*	0.36

^{a} above the room temperature

Table 3 Ionic conductivity σ_{imp}, lithium cation transference numbers t_{Li+} for the different ionogel and neat ES.

Sample	$\sigma_{imp}^{\ a}$	t_{Li+}
ES	$1.4 \cdot 10^{-3}$	0.09
ES/SiO$_2$ = 1	$1.7 \cdot 10^{-3}$	0.02
ES/SiO$_2$ = 0.5	$0.8 \cdot 10^{-3}$	0.14
ES/SiO$_2$ = 0.25	$0.05 \cdot 10^{-3}$	0.14

^{a} at 20°C.

and its lower temperature since its quenches the crystallization.

This non-Arrhenius behavior is well described by the Vogel-Tamman-Fulcher (VTF) equation. In this equation (Eq. 2), T_0 is the so called ideal T_g, at which all molecular mobilities vanishes, also named Vogel temperature.

$$\sigma = \sigma_0 \, \exp\left[- B/(T - T_0)\right] \tag{2}$$

Based on this model, pre-exponential factor σ_0, B and T_0 parameters were obtained (Fig. 3B) and their values are summarized in Table 2. The fit was performed within a broad temperature range, in the liquid region, well above the glass transition temperature T_g because of the possible crystallization. The results of the fittings show that these parameters are affected by the ES/SiO$_2$ ratio and therefore by the pore size. It has to be point out that data for the ES/SiO$_2$ = 0.25 ionogel did not allow obtaining fitting parameters with as good reliability as for others fittings.

Lithium cation transference numbers (t_{Li+}) were measured using the D.C. polarization method with neat ES and with different ionogels; the results are presented Table 3. Lithium cation transference number increases when the ES/SiO$_2$ ratio decreases, to reach up to 0.14 with ionogel ES/SiO$_2$ = 0.25. This highlights that a smaller pore size improves t_{Li+}.

^{7}Li MAS NMR spectra are presented Fig.4. The spectrum of neat, liquid, ES as well as those of solid ionogels were recorded without spinning. The linewidth observed herein for ionogels remains below 300Hz for all ES/SiO$_2$ ratio, as already reported elsewhere.[8] Although broader than that measured for the liquid ES, ionogels linewidths are clearly more than one order of magnitude narrower than the typical solid state linewidth observed for Li nuclei (several 1000Hz). This result confirms the dynamic environment of Li and the liquid-like behaviour of ES in ionogels presented in previous works.[6] The FWHM of ES and of the ionogels presented Table 4, without any applied electric field, show the expected evolution. As FWHM is linked to the dynamics of species, a decrease in FWHM that is simultaneous
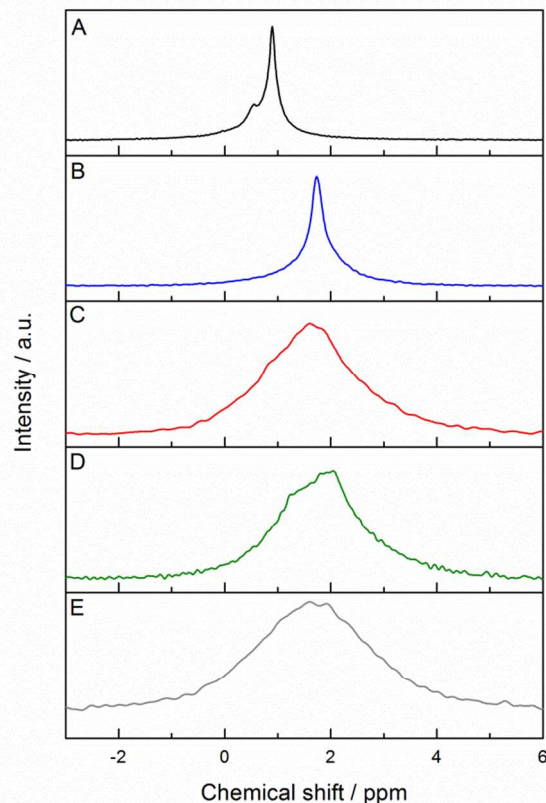
Fig. 4 7Li MAS NMR spectra recorded at room temperature without rotation of (A) neat ES, (B) ionogel ES/SiO$_2$ = 1, (C) ionogel ES/SiO$_2$ = 0.5, (D) ionogel ES/SiO$_2$ = 0.25 and (E) ES with preformed SiO$_2$.

Table 4 ^{7}Li MAS NMR FWHM and δLi$^+$ for ES, different ionogels and a mixture of ES with SiO$_2$.

Sample	FWHM [ppm]	δ_{Li+} [ppm]
ES	0.22	0.9
ES/SiO$_2$ = 1	0.51	1.75
ES/SiO$_2$ = 0.5	1.78	1.62
ES/SiO$_2$ = 0.25	1.69	1.81
ES + SiO$_2$ ^{a}	2.42	1.65

^{a} ES/SiO$_2$ molar ratio is 1

with the increase of overall ES/SiO$_2$ ratio, indicates an overall faster dynamics for a higher ES/SiO$_2$ ratio. Thus, in the absence of any electric field, the increase of confinement leads to a decrease in the overall dynamics of lithium. In addition, the ^{7}Li chemical shift measured for ionogels (approx. 1.7ppm) is different from that of ES alone (0.9ppm) but is similar to the chemical shift observed for the mixture of ES with preformed SiO$_2$. Thus, the ^{7}Li resonance rising between 1.6 and 1.8ppm can be tentatively assigned to Li nuclei at a silica interface neighbourhood.

The Raman spectra of the neat ES and in the spectra range 725-760 cm^{-1} are presented Fig. 5. The range around 740 cm^{-1} is characteristic of the symmetric breathing mode of the TFSI anion

Table 5 Thermal- and fragility- to-porosity relationship

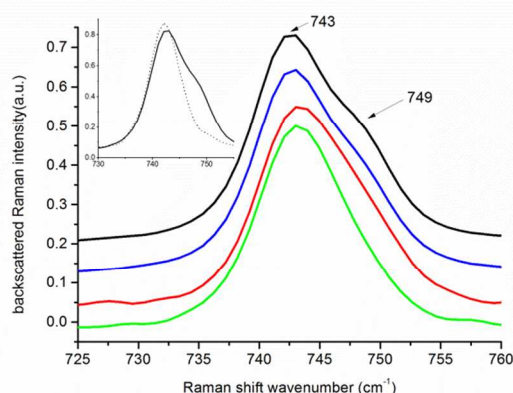| Sample	T_g [K]	T_o/T_g	$\Delta_m H$ [J.g^{-1}]	$\Delta_m H$ bulk-like [%mol]	D	Schematic pore texturation
ES	191	0.97	28.4	100	3.4	
ES/SiO$_2$ = 1	194	0.96	20.9	84	3.0	
ES/SiO$_2$ = 0.5	199	1.00	1.41	6	2.4	
ES/SiO$_2$ = 0.25	202	*1.11*	0.37	2	1.8	

Fig. 5 Raman spectra recorded at room temperature of (dotted line, insert) Pyr13 TFSI without lithium cation, (black, insert and main) neat ES, (blue) ionogel ES/SiO$_2$ = 1, (red) ionogel ES/SiO$_2$ = 0.5 and (green) ionogel ES/SiO$_2$ = 0.25.

involving the CF$_3$ bending and the S-N stretching movements. This band allows distinguishing between Li-coordinated TFSI anion and non Li-coordinated TFSI anion.[23] The shoulder appearing in the insert is due to coordination of lithium cation to TFSI anion. It appears also in the ionogel with ES/SiO$_2$ = 1, and decreases clearly when ES/SiO$_2$ decreases. This is a direct evidence of the decrease of the TFSI-Li coordination when pore size is decreasing.

Discussion

All information presented above is summarized in Table 5. Overall, the behavior of the confined IL is related to the fragility index D.[24,25] The fragility index D is derived from the VTF equation (Eq. 3) and its value is inversely proportional to the fragility of the liquid.

$$B = D.T_0 \qquad (3)$$

Fragility is a measure of the thermal sensitivity of the liquid structure. A fragile liquid collapses under weak perturbations and leads to structural re-arrangement. Thus a fragile liquid shows fast dynamical re-arrangement featured by short relaxation times τ, non-Fickian diffusion, giving rise to non-Arrhenius behaviour.

A low value on the fragility index corresponds to weak molecular interactions, while a high value corresponds to strong molecular interactions.[18,26] Thus, fragility is related to molecular mobility with its correlative effect on ionic conductivity and viscosity: far above T_g, as here around 100K above T_g, a small D value implies a high ionic mobility and a low viscosity. In ILs, the interactions between ions results in their high cohesive energy. The liquid phase typically consists of highly associated anions-cations, in addition to aggregated areas with varying spatial extension and life-time.[19,27] It is here worth to point out that in-depth understanding of ions pair interactions in ILs is still under debate.[28-32] Upon confinement of ILs in proximity to polar silica surfaces (silanols with multiple orientations forming dynamic hydrogen bonds), layering was observed,[30] with either cations or anion preferentially interacting with the surface.[33,34] It has to be pointed out that interface effect shows similarities with low dimensionality behaviour which was shown to produce enhanced charge transport.[35] For the ionogel, the decrease of the ES/SiO$_2$ ratio shows a decrease of the D parameter, along with a decrease of pore size and an increase of the specific surface per mol of confined ES. This suggests that a smaller porosity, as low as ~8 nm, leads to an increase of IL fragility in ionogel (small D index). It appears that interaction with the host matrix, *i.e.* interfaces, breaks down aggregated regions which are found systematically in ILs. The lowering of anion-cation association should be associated with an increase of the ionicity. Consequently, ionogels with low ES/SiO$_2$ values have low D values and are "fragile" ionogels. More precisely, the confined ILs are more fragile, and present higher molar (*vs.* IL amount) conductivity and lower density and viscosity, locally at silica interface. This results in a higher ionicity. Moreover, increasing T_0/T_g also show the increasing fragility when decreasing ES/SiO$_2$ ratio.[36]

The lithium environment and its dynamics in ionogel were observed by ^{7}Li NMR, Raman spectroscopy and by lithium transference numbers measurements. For the lithium cation, the NMR chemical shift shows that the lithium is present, but not immobilized, at the surface of the silica. The dynamics of the silanol groups could help creating for Li$^+$ cation a diffusion path at the interface. Since the synthesis is carried out with formic acid, the silica surface is slightly charged, due to a surface made of only few silanolates and mainly silanols. The lithium ion transference number shows an increase in line with the decrease of the pore size. Such increase of the transference number could be due simultaneously to an increase in the ionicity of IL at the

wall neighbourhood, as explained above, as well as to surface silanolates creating highly preferential diffusion pathways for lithium cations. The intensity of this phenomena is further heightened as the fragility of the IL is increased by the decrease
[5] of the pore size and the increase of the surface relatively to IL amount (t_{Li+} = 0.09 and 0.14 for ES/SiO$_2$ = 1 and ES/SiO$_2$ = 0.25 *resp.*). Other studies have shown that silica particles results in an increase in ionic conductivity.[37,38] Similar behaviour has been reported for a molecular solvent that contains pairs of lithium
[10] cation and counter-anion, which dissociate efficiently at the polymer or acidic SiO$_2$ interface.[39-41] ^{7}Li NMR shows the vicinity of lithium cation and silica, and Raman shows that TFSI anion is less coordinated with lithium when confinement in silica host network occurs. Consequently, a segregation of lithium cations,
[15] preferentially at the silica interface, is obvious and its migration, participates to the relatively high t_{Li+} transference number.

Conclusions

It is shown here that confining ILs within silica host networks enhances their fragility, resulting in improved ion transport.
[20] Fragility, short relaxation times, low viscosity, and good ionic conductivity are all related to the ES/SiO$_2$ interface. Ionogels with lower ES/SiO$_2$ ratios present the smallest pore size and show the best performances. Probing specifically lithium cation and TFSI anion *resp.* with NMR and Raman spectroscopies gives
[25] direct evidences of ions segregation within silica based ionogels. Confinement of ILs leads at interfaces to some breakdown of aggregated, structured regions that are found systematically in bulk ILs. This "destructures" aggregated pairs or domains in the ILs. Solid ionogels, specifically with smaller pores size, strongly
[30] display this effect, which are coupled with percolation of their bicontinuous interfaces. This makes these materials very competitive solid electrolytes, since they provide a route lowering density and viscosity of ILs, and enhancing their conductivity. This general approach to enhance conductivity can be applied to
[35] many all-solid devices, including supercapacitors and lithium batteries.

Acknowledgements

Notes and references

[a] *Institut des Matériaux Jean Rouxel (IMN) – CNRS – Université de Nantes - 2, rue de la Houssinière, B.P. 32229, 44322 Nantes Cedex 3, France. Fax: +33 240 373 995; Tel: +33 240 373 919 ; E-mail:*
[45] *jean.lebideau@cnrs-imn.fr*

1   J. P. Hallett, T. Welton, *Chem. Rev.,* 2011, **111**, 3508.
2   J.G. Huddleston, R.D. Rogers, *Chem. Comm.,* 1998, **0**, 1765.
3   A. Lewandowski, A. Swiderska-Mocek, *J. Power Sources*, 2009, **194**, 601.
[50] 4   M. Armand, F. Endres, D. R. MacFarlane, H. Ohno, B. Scrosati, *Nat Mater,* 2009, **8**, 621.
5   J. Le Bideau, L. Viau, A. Vioux, *Chem.Soc. Rev.*, 2011, **40**, 907.
6   J. Le Bideau, P. Gaveau, S. Bellayer, M.-A. Neouze, A. Vioux, *Phys. Chem. Chem. Phys.*, 2007, **9**, 5419.
[55] 7   K. Ueno, M. Kasuya, M. Watanabe, M. Mizukami, K. Kurihara, *Phys. Chem. Chem. Phys.*, 2010, **12**, 4066.
8   T. Echelmeyer, H.W. Meyer, L. van Wullen, *Chem. Mater.*, 2009, **21**, 2280.
9   J. Le Bideau, J.-B. Ducros, P. Soudan, D. Guyomard, *Adv. Funct.
[60] Mater.*, 2011, **21**, 4073.
10 M. J. Monteiro, F. F. C. Bazito, L. J. A. Siqueira, M. C. C. Ribeiro, R. M. Torresi, *J. Phys. Chem. B*, 2008, **112**, 2102.
11 A.M. Smith, K.R.J. Lovelock, N.N. Gosvami, P. Licence, A. Dolan, T. Welton, S. Perkin, *J. Phys. Chem. Letters,* 2013, **4**, 378.
[65] 12 W. Xu, C.A. Angell, *Science,* 2003, **302**, 422.
13 M. Yoshizawa, W. Xu, C.A. Angell, *J. Am. Chem. Soc.*, 2003, **125**, 15411.
14 W. Xu, E.I. Cooper, C.A. Angell, *J. Phys. Chem. B*, 2003, **107**, 6170.
15 K.J. Fraser, E.I. Izgorodina, M. Forsyth, J.L. Scott, D.R. MacFarlane,
[70] *Chem. Comm.*, 2007, 3817.
16 D.R. MacFarlane, M. Forsyth, E.I. Izgorodina, A.P. Abbott, G. Annat, K. Fraser, *Phys. Chem. Chem. Phys.*, 2009, **11**, 4962.
17 H. Tokuda, K. Hayamizu, K. Ishii, M.A.B.H. Susan, M. Watanabe, J. *Phys. Chem. B*, 2004, **108**, 16593.
[75] 18 A. Noda, K. Hayamizu, M. Watanabe, *J. Phys. Chem. B*, 2001, **105**, 4603.
19 H. Tokuda, S. Tsuzuki, M.A.B.H. Susan, K. Hayamizu, M. Watanabe, *J. Phys. Chem. B*, 2006, **110**, 19593.
20 C.-M. Wu, S.-Y. Lin, K.-Y. Kao, H.-L. Chen, *J. Phys. Chem. C*,
[80] 2014, **118**, 17764; C.-M. Wu, S.-Y. Lin, H.-L. Chen, *Micropor. Mesoporo. Mater.*, 2012, **156**, 189.
21 N. Borisenko, R. Atkin, A. Lahiri, S. Zein El Abedin, F. Endres, *J. Phys.: Condens. Matter.*, 2014, **26**, 284111.
22 M. Waechtler, M. Sellin, A. Stark, D. Akcakayiran, G. Findenegg, A.
[85] Gruenberg, H. Breitzke, G. Buntkowsky, *Phys. Chem. Chem. Phys.*, 2010, **12**, 11371.
23 J. Pitawala, J.-K. Kim, P. Jacobsson, V. Koch, F. Croce, A. Matic, *Faraday Discuss.*, 2012, **154**, 71.
24 C.A. Angell, *J. Non-Cryst. Solids*, 1991, **131-133**, 13.
[90] 25 C.A. Angell, *Science*, 1995, **267**, 1924.
26 J.L. Ndeugueu, M. Ikeda, M. Aniya, *Solid State Ionics,* 2010, **181**, 16.
27 D. R. MacFarlane, M. Forsyth, E. I. Izgorodina, A. P. Abbott, G. Annata, K. Fraser, *Phys. Chem. Chem. Phys.*, 2009, **11**, 4962.
[95] 28 M. A. Gebbie, M. Valtiner, X. Banquy, E. T. Fox, W. A. Henderson, J. N. Israelachvili, *PNAS*, 2013, **110**, 9374.
29 M. V. Fedorov, A. A. Kornyshev, *Chem. Rev.*, 2014, **114**, 2978.
30 A. A. Lee, D. Vella, S. Perkin, A. Goriely, *J. Chem. Phys.*, 2014, **141**, 094904.
[100] 31 H. Weingärtner, *Angew. Chem. Int. Ed.*, 2008, **47**, 654.
32 A. M. Fernandes, M. A. A. Rocha, M. G. Freire, I. M. Marrucho, J. A. P. Coutinho, L. M. N. B. F. Santos, *J. Phys. Chem. B*, 2011, **115**, 4033.
33 M. P. Singh, R. K. Singh, S. Chandra, *J. Phys. Chem. B*, 2011, **115**,
[105] 7505.
34 N. Sieffert, G. Wipff, *J. Phys. Chem. C*, 2008, **112**, 19590.
35 C. Iacob, J. R. Sangoro, W. K. Kipnusu, R. Valiullin, J. Kärger, F. Kremer, *Soft Matter*, 2012, **8**, 289.
36 I. M. Hodge, *J. Non-Cryst. Solids*, 1996, **202**, 164.
[110] 37 Y. Aihara, G.B. Appetecchi, B. Scrosati, K. Hayamizu, *Phys. Chem. Chem. Phys.,* 2002, **4**, 3443.
38 Y. Tominaga, S. Asai, M. Sumita, S. Panero, B. Scrosati, *J. Power Sources*, 2005, **146**, 402.
39 C. Pfaffenhuber, M. Göbel, J. Popovic, J. Maier, *Phys. Chem. Chem.
[115] Phys.*, 2013, **15**, 18318.
40 N. Buchtova, A. Guyomard-Lack, J. Le Bideau, *Green Chem.*, 2014, **16**, 1149.
41 A. Guyomard-Lack, J. Abusleme, P. Soudan, B. Lestriez, D. Guyomard, J. Le Bideau, *Adv. Energ. Mater.*, 2014, **4**, 1301570.

[120]